Interfacial Synthesis of Nylon-6.6 and Its Modification with Silver-Based Nanoparticles at the Electrified Liquid-Liquid Interface

Karolina Kowalewska[a], Dr. Karolina Sipa[a], Katarzyna Kaczmarek[a], Prof. Sławomira Skrzypek[a], Dr. hab. Lukasz Poltorak[a*]

a. *Department of Inorganic and Analytical Chemistry, Electroanalysis and Electrochemistry Group, Faculty of Chemistry, University of Lodz, Tamka 12, 91-403 Lodz, Poland.*

***Corresponding author:** lukasz.poltorak@chemia.uni.lodz.pl*

Abstract

In this work, the synthesis of Nylon-6.6 together with silver nanoparticles (presumably Ag_2O, Ag NPs) was carried out at a polarized liquid-liquid interface (LLI). The reduction of silver ions to Ag-NPs was driven by an electrochemically controlled electron transfer reaction between silver cations initially dissolved in the aqueous phase and ferrocene species present in the organic phase. The formation of Ag_2O is assumed to originate from Ag^+ precipitation to AgOH further converted into Ag_2O. The polyamide formation was derived from the interfacial polycondensation reaction happening between 1,6-diaminohexane and adipoyl chloride. We have studied the possibility to form given material simultaneously (interfacial polycondensation and Ag^+ reduction occurring in one step) and sequentially (electrochemical Ag^+ reduction by ferrocene from the organic phase was performed after polyamide deposition). The Ag-based NPs-polyamide material has been synthesized at the macroscopic and microscopic LLI. As the support for the latter, we have used fiberglass membranes. The resulting material was characterized by infra-red (IR) spectroscopy and scanning electron microscopy (SEM).

Keywords: Electrochemistry; Interfacial electron transfer; Interfacial polycondensation; ITIES; Materials Science:

Introduction

Electrochemistry at the polarized liquid-liquid interface (LLI), also known as the interface between two immiscible electrolyte solutions (ITIES), allows the study of interfacial charge transfer reactions in the form of ions or electrons crossing soft junctions.[1,2] The defect-free ITIES system is self-healing, renewable, discontinuous, and also modifiable.[3] LLI takes the shape of the support and thanks to its asymmetric properties it can separate the chemical species based on their affinity to adjacent phases. ITIES based systems can be studied with all available electrochemical techniques.[2,4,5] One of the possible directions further exploring these unique systems is the interfacial synthesis of materials. LLI

should be used to explore new possibilities allowing the interfacial materials synthesis. When combined with the electrochemical polarization, not only we can control the polycondensation reactions but also further modify the interface with other objects brining desired functionality. Finally, due to asymmetric properties of the biphasic junction we can obtain Janus materials that are very difficult or even impossible to prepare in monophasic systems.

The LLI can exist in different sizes, as defined by Liu *et al.,* the nano-, micro-, and macroscopic scales.[6] The latter can be referred to as a conventional system having at least several millimeters in diameter (e.g. conventional voltammetric cell with two Luggin capillaries defining the position of the soft junction). LLI miniaturization can be achieved with appropriate support (e.g. in a form of membranes or capillaries) or adequate processing (e.g. intensive mixing). The membranes used to create nano- or micro-interfaces are usually made out of patterned supports or materials displaying intrinsic porosity.[7] Single pore ITIES can be prepared from pulled glass capillaries,[8] a pore formed in a glass pipette after dissolving a metal wire embedded within the glass casing,[9] or fused silica microcapillaries.[3] Miniaturized liquid boundaries provide additional stability to the LLI whereas the solid surrounding of the soft junction may serve as the support for the interfacially formed deposits.

The modification of the LLI can be carried out either *in-situ* or *ex-situ*. According to the first methodology, the preformed modifier is added to one phase followed by its precipitation at or adsorption to the soft junction. This approach was used to decorate the LLI with a variety of objects such as metallic nanoparticles,[10] carbon nanotubes,[11] silica spheres[12] etc. The *in situ* modification is derived from the interfacial ion or electron transfer triggering the reaction(s) whose product(s) resided within the interfacial region in a form of solid/soft deposits.[13] In this respect, metallic nanoparticles can be formed within the interface originating from the cationic precursor reduction (initially dissolved in the aqueous phase) by the organic phase soluble electron donor (usually ferrocene and its derivatives).[14–17] Another example is electrochemically controlled interfacial polymerization either derived from the electron[18–21] or ion transfer reaction.[22] Sol-gel processing in a biphasic environment can also be studied or controlled using electroanalytical techniques.[23–26] The modification following *ex-situ* methodology is based on the pre-formed objects or molecular assemblies (metallic particles, carbon-based materials, proteins, surface-active species) that adsorb to the LLI. [11,27–31] Such assemblies found applications in heterogeneous electrocatalysis (especially when metallic nanoparticles are used)[32] and for biomimetic studies (e.g. interfacial behavior of proteins).[33–36]

In this work, for the first time, we have studied the *in-situ* LLI modification with nylon-6,6 and Ag-based NPs. Interfacial polycondensation of the polyamide was based on our previously reported work

whereas the Ag-based NPs were obtained via heterogeneous and electrochemically controlled reduction of Ag-complex (formed in the presence of 1,6-diaminohexane) initially dissolved in the aqueous phase by the electron-donating ferrocene species dissolved in the organic phase and probably chemical reactions (formation of AgOH and Ag_2O) expected to occur at pH = 11. The interfacial formation of both materials (nylon-6,6 and Ag-based NPs) followed two processing methodologies: (i) Ag-based NPs deposition during polyamide formation and (ii) Ag-based NPs deposition after the initial deposition of a polyamide film. The developed material was initially formed at the macroscopic and planar LLI. Further utilization of the soft junction support in the form of the fiberglass membrane facilitated the obtained material processing. Our platform was investigated with cyclic voltammetry, scanning electron microscopy, and infra-red spectroscopy. The aim of this work is to define the possibility to control electrochemically the interfacial polycondensation reactions aiming at the formation of polyamide materials further modified with functional objects (Ag-base NPs display antibacterial properties).

Methods and materials

Chemicals and materials

Sodium sulfate (Na_2SO_4, anhydrous, for analysis, POCh) was used to prepare an aqueous phase at pH = 11. The pH was adjusted with 0.1 M sodium hydroxide (NaOH, for analysis, ChemPur). 1,6-diaminohexane (1,6-DAH, ≥99.5%, Acros Organics), adipoyl chloride (AC, 98%, Alfa Aesar), silver nitrate ($AgNO_3$, ≥99.8%, Fisher Chemical), sodium nitrate ($NaNO_3$, for analysis, ChemPur) and ferrocene (Fc, 98%, Acros Organics) were used as received. The organic phase electrolyte $BTPPA^+TPBCl^-$ (Bis(triphenylphosphoranylidiene)ammonium tetrakis(4-chlorophenylborate)) was synthesized using bis(triphenylphosphoranylidene)ammonium chloride ($BTPPA^+Cl^-$, 97%, Sigma-Aldrich) and potassium tetrakis(4-chlorophenyl)borate ($KTPB^+Cl^-$, ≥98%, Sigma-Aldrich) via methatesis reaction. The organic phase was prepared by dissolving a proper amount of $BTPPA^+TPBCl^-$ in 1,2-dichloroethane (1,2-DCE, for analysis, POCH,). Fiberglass membranes (glass microfiber discs, diameter: 47.0 mm, thickness: 0.2 mm, Ahlstrom Munksjo) glued with silicone to glass tubes were used to create miniaturized liquid-liquid interfaces. All experiments were performed using demineralized water (Hydrolab system, Poland).

Electrochemical experiments

Electrochemically controlled synthesis and modification of polyamide material were performed in a macroscopic voltammetric glass cell (interface radii equal to 0.7 cm) equipped with four electrodes: two $Ag/AgSO_4$ reference electrodes and two Pt counter electrodes. The reference electrodes were prepared by applying anodic potential to the silver wire immersed into 1M H_2SO_4

solution for 5 minutes. The micro-ITIES systems were prepared by cutting a fiberglass membrane using a scalpel knife. This was then attached to a glass tube with silicone sealant. The created system was filled with the organic phase and immersed in the aqueous phase. Electrode configuration was analogical to macroscopic equivalent. The hardware used during our experiments was Autolab 302N (Metrohm). The plotted cyclic voltammograms are either given as the current in function of the Galvani potential difference ($\Delta\phi$) or the potential applied using the external power supply – potentiostat. For the latter, the x-axis label reads as "Potential / V". Whenever, the $\Delta\phi$ is given, the x-axis were calibrated using the standard Galvani potential of the TMA^+ cation transfer, equal to 160 mV.[5] Other curves are not calibrated due to the lack of a good internal reference potential difference point. A number of interfacial charge transfer reactions happening in the system overlay (additionally due to high concentration of the reagents), and hence, the common practice relaying on model reference ion addition failed. The iR-compensation was not applied during the experiments.

Infrared spectroscopy

Materials synthesized at the ITIES were collected and analyzed with infra-red spectroscopy (Nexus FT-IR by Thermo Nicolet spectrometer) in transmission mode. Before analysis, all samples were mixed with KBr and the pastille was formed.

Scanning Electron Microscopy

The scanning electron microscopy (SEM, a Phenom G2 Pure, FEI Company, the Netherlands) was used to examine the surfaces of bare and modified polyamide material extracted from macroscopic cells or being a part of microporous fiberglass membranes used as an ITIES support. During analysis, the samples were fixed on an SEM pin stub using copper tape. SEM images were acquired at a magnification of 250-2500x using a high-sensitivity backscattered electron detector operating at an accelerating voltage of 5 kV.

Result and discussion

Fig. 1A shows the macroscopic cell used during ITIES modification with polyamide film and polyamide film decorated with Ag NPs. On either scale (macroscopic and microscopic), ITIES was polarized using a four-electrode configuration with two platinum counter electrodes one placed in the aqueous and the second in the organic phase. Hydrophilic background electrolyte (Na_2SO_4), $AgNO_3$, and/or diamine were always initially present in the aqueous phase whereas the organic phase was a solution of hydrophobic salt (BTPPATPBCl), adipoyl chloride, and/or ferrocene. In such a configuration we can distinguish a few major reactions governing the interfacial formation of studied deposits. Fig. 1B indicates simple ion transfer reactions of Ag^+ and NO_3^- which can be recorded within the available

voltammetric potential window. Positive currents will be defined as the Ag^+ transfer from the aqueous to the organic phase. Although for this cation the scheme (Fig. 1B) depicts a simple ion transfer reaction, Sherburn *et al.* have found that the interfacial transfer of Ag^+ is affected by the nature of the organic phase background electrolyte anion shifting its Galvani potential of ion transfer from -0.01 V for tetraphenylborate anion to 0.17 V for tetrakis(4-chlorophenyl)borate.[37] This indicates that the interfacial transfer of Ag^+ is additionally facilitated by the negatively charged hydrophobic anions dissolved in the organic phase. Transfer of NO_3^- ($\Delta_{org}^{aq}\phi'_{NO_3^-} = -0.351\ V$)[5] from the aqueous to the organic phase will be recorded as the negative current. The interfacial polycondensation of two monomers, 1,6-DAH from the aqueous phase and AC from the organic phase is shown in Fig. 1C. Previously, we have shown that at an appropriate pH value assuring the existence of 1,6-DAH in a partially protonated form we can introduce the electrochemically controlled step during interfacial polyamide formation. We have concluded that the partially protonated 1,6-DAH undergoing transfer from the aqueous to the organic phase can react with the acyl chloride group of the AC. Under such conditions, the resulting polyamide film formation was accelerated.[38] Fig 1D schematically depicts the interfacial electron transfer reaction between ferrocene (Fc) species from the organic phase and Ag^+ cations dissolved in the aqueous phase. Once the appropriate Galvani potential difference is applied to the ITIES the electron-donating Fc is being oxidized to ferrocenium cation (Fc^+) whereas Ag^+ is reduced to Ag^0 which resides at the ITIES in a form of Ag NPs. Interfacial reduction of Ag^+ to Ag^0 can be achieved with other electron donating hydrophobic reducing chemical species (e.g. ferrocene derivatives[39] or N-phenylpyrrole[40]). Finally, as shown in Fig. 1E, Fc^+ formed during Ag NPs formation is also interfacially active and can be transferred from the organic to the aqueous phase below its $\Delta_{org}^{aq}\phi'_{Fc^+}$ which was reported to be 0.041 V.[41] Consequently, when all reagents needed to form polyamide film decorated with Ag NPs are present in biphasic system a number of mutually interconnected reactions may occur as shown in Fig. 1F.

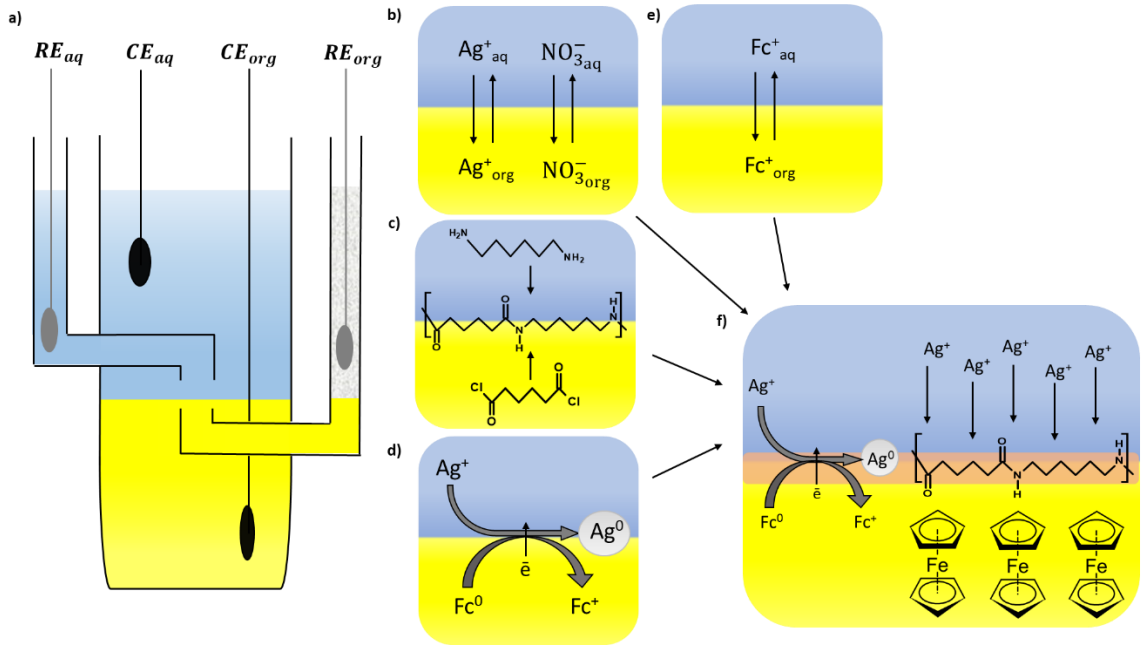

Fig. 1 A – Scheme showing four-electrode electrochemical cell used for the simultaneous deposition of Ag NPs and polyamide film (RE – reference electrode; CE – counter electrode; aq – the aqueous phase; org – the organic phase). Reactions happening in the cell during interfacial modification: B – simple ion transfer of Ag^+ and NO_3^- happening across the LLI; C – interfacial polycondensation happening between 1,6-DAH and AC resulting in the polyamide formation; D – interfacial electron transfer reaction from the organic phase to the aqueous phase originating from the reduction of Ag^+ to metallic Ag and ferrocene (Fc) oxidation to ferrocenium cations (Fc^+); E – simple ion transfer of Fc^+ across the LLI. F – is the scheme summarizing key interfacial charge transfer reaction leading to the formation of a polyamide film decorated with Ag NPs.

Fig. 2A shows cyclic voltammograms (CVs) recorded before and after addition of $AgNO_3$ to the aqueous phase (pH = 7) at concentration equal to 100 µM. The series of CVs recorded at different [$AgNO_3$] are available as Fig. S1A. In the absence of $AgNO_3$ in the aqueous phase, the available potential window was limited by the Na^+ transfer from the aqueous to the organic phase ($\Delta^{aq}_{org}\phi^0_{Na^+}$ = 0.591 V; positive current on the more positive potential side)[5] and SO_4^{2-} transfer from the aqueous to the organic phase ($\Delta^{aq}_{org}\phi^0_{SO_4^{2-}}$ = -0.509 V; negative current on the less positive potential side)[42] – see the red curve on Fig. 2A. We have used Ag/Ag_2SO_4 as the aqueous phase reference electrodes[43] immersed into Na_2SO_4 solution. This was possible as we did not observe any precipitation of the Ag_2SO_4 since the concentration of used reagents were always below its molar solubility ($K_{sp} = 1.2 \cdot 10^{-5}$).[43] The presence of Ag^+ and NO_3^- in the aqueous phase resulted in the appearance of two extra pairs of signals. The negative end of the potential window was attributed to NO_3^- transfer as further confirmed by the increasing positive and negative currents in the potential range from -0.5 to -0.1 V recorded for the

increasing concentration of $NaNO_3$ added to the aqueous phase (see Fig. 2C and 2D and Fig. S1B from supporting information). Fig. 2B shows the positive and negative peak current attributed to the Ag^+ interfacial transfer plotted in function of the $AgNO_3$ concentration. Obtained dependency deviates from the linear calibration curve expected for the simple ion transfer reaction. The ratio of the slopes for the first three studied concentrations obtained for the positive ($3.478 \cdot 10^{-7}$ $A \cdot M^{-1}$) and negative ($-3.958 \cdot 10^{-7}$ $A \cdot M^{-1}$) signals is equal to 0.88 which deviates from unity expected for fully reversible reaction. These observations are in line with what was reported by Sherburn *et al.* who indicated that Ag^+ transfer across the LLI is additionally facilitated by the organic phase background electrolyte salt anion – here TPBCl.[37] Occasionally, we were also recording current spikes (see negative potential ranges in Fig. 2A and Fig. S1A and Fig. S1B) characteristic for the phenomena studied by the group of Kakiuchi – electrochemical instability.[44,45] Most probably, the applied negative potentials are enough to trigger interfacial emulsification. Formed droplets of either aqueous phase containing background electrolyte ions or loaded organic phase release the cargo upon the collision with the eLLI followed by interfacial fusion.[46]

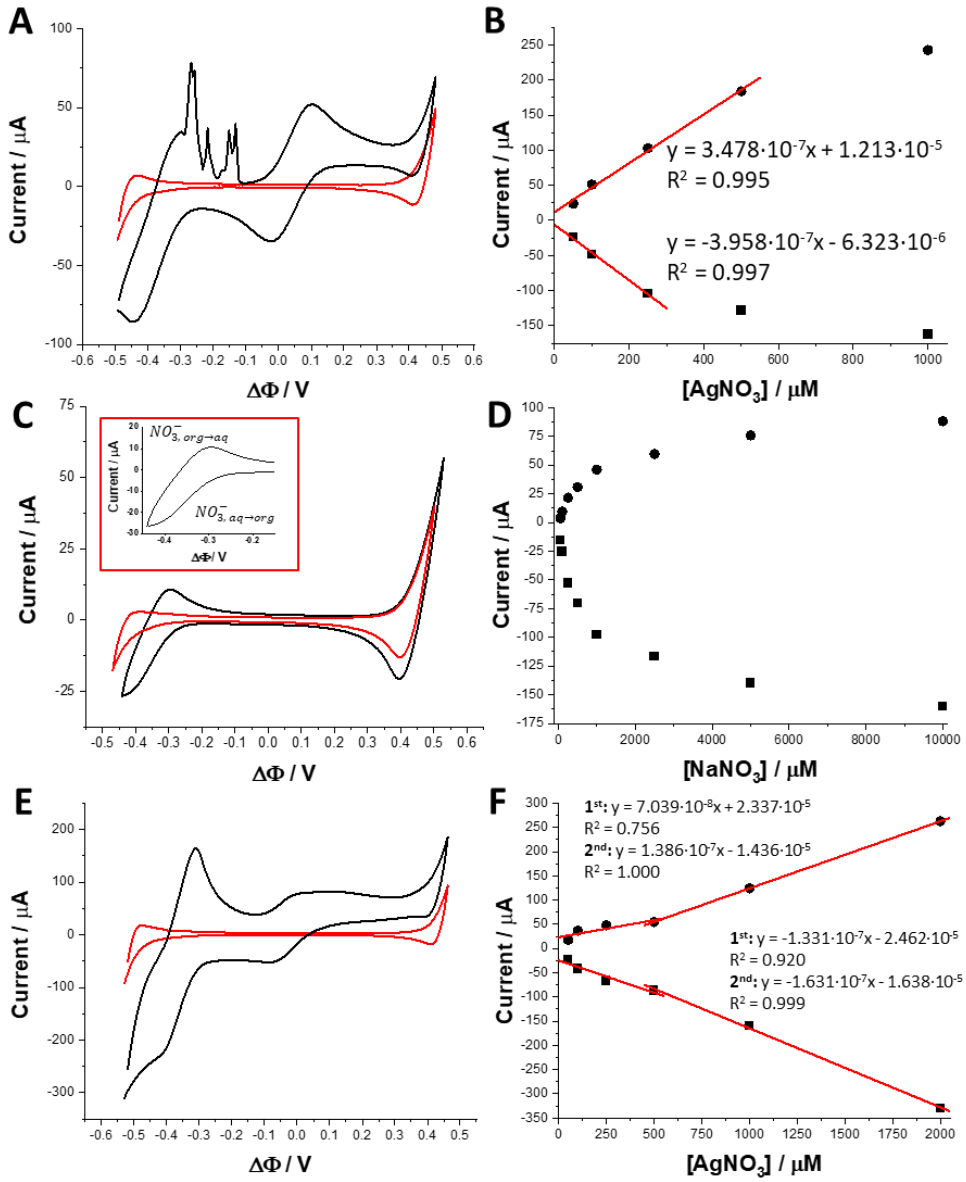

Fig. 2. Cyclic voltammograms (A, C, and E) recorded at different compositions of the aqueous and the organic phase. A – The aqueous phase: 10 mM Na_2SO_4 (pH = 7) with [$AgNO_3$] = 100 µM; the organic phase: 5 mM BTPPATPBCl in 1,2-DCE. C - The aqueous phase: 10 mM Na_2SO_4 (pH = 7) with [$NaNO_3$] from 100 µM; the organic phase: 5 mM BTPPATPBCl in 1,2-DCE. Inset: [$NaNO_3$] = 100 µM. All CVs were recorded at 20 mV·s^{-1}. E – The aqueous phase: 10 mM Na_2SO_4 (pH = 7) with [$AgNO_3$] =500 µM; the organic phase: 10 mM Fc and 5 mM BTPPATPBCl in 1,2-DCE. B – Calibration curve plotted based on CVs from section A for the signals corresponding to Ag^+ transfer (from -0.1 till 0.3 V). D – Calibrations curves plotted based on CVs from section C for the limiting current on the less positive potential window side. F – Calibration curves plotted based on CVs from section E for the signals recorded in the range from -0.2 till 0.2 V.

The interesting appearance of the recorded voltammetric curves was obtained when the organic phase composition was enriched by 10 mM Fc – see Fig. 2E. Here, the CVs were recorded in the presence and the absence of $AgNO_3$. CVs recorded for the increasing concertation of $AgNO_3$ in the presence of Fc in the organic phase are available as Fig. S1C. First pair of peaks with the $\Delta_{org}^{aq}\phi_{1/2}$ being equal to around -0.35 V was attributed to the transfer of NO_3^-. The negative signal with a peak maximum at -0.44 V (recorded at [$AgNO_3$] = 500 µM) is due to NO_3^- transfer from the aqueous to the organic phase.

Signals with $\Delta_{org}^{aq}\phi_{1/2}$ at around -0.05 V are complex and the governing currents are a mixture of a few processes, this is Ag^+ interfacial transfer (see eq. 1), heterogenous electron transfer between Fc and Ag^+ (see eq. 2), and the interfacial transfer of Fc^+ (see eq. 3) and charge balancing anion (see eq. 4; signals recorded below -0.15 V):[47]

$$Ag_{aq}^{+} \rightleftarrows Ag_{org}^{+} \quad (1)$$

$$Fc_{org} + Ag_{aq}^{+} + NO_{3,aq}^{-} \rightarrow Fc_{org}^{+} + Ag_{LLI}^{0} + NO_{3,org}^{-} \quad (2)$$

$$Fc_{org}^{+} \rightleftarrows Fc_{aq}^{+} \quad (3)$$

$$NO_{3,aq}^{-} \rightleftarrows NO_{3,org}^{-} \quad (4)$$

Reactions 1 and 2 can be observed as the elongated positive peak (see Fig. 2E) being a mixture of a current originating from the interfacial Ag^+ reduction (first signal forming a clear peak at 0 V), and Ag^+ transfer to the organic phase (shoulder of the positive signal that can be noticed in the potential difference range from 0.1 V till 0.3 V) where it can also be reduced to Ag^0 (see eq. 5 and eq. 6). Also, the reduction of Ag^+ to metallic Ag^0 is associated with the formation of interfacially active Fc^+ that may give additional ionic current features (eq. 3) that are expected to occur at around $\Delta_{org}^{aq}\phi'_{Fc^+}$= – 0.016 V.[48] Even in the absence of $AgNO_3$, the signal with a small intensity was observed at around 0 V which corresponds to the Fc^+ transfer formed upon spontaneous oxidation (the aqueous phase was not deprived from the oxygen during the experiments).[49–51]

$$Fc_{org} + Ag_{org}^{+} \rightarrow Fc_{aq}^{+} + Ag_{LLI}^{0} \quad (5)$$

$$Fc_{org} + Ag_{org}^{+} + NO_{3,aq}^{-} \rightarrow Fc_{org}^{+} + Ag_{LLI}^{0} + NO_{3,org}^{-} \quad (6)$$

The recorded positive signal (Fig. 2E or Fig. S1C) with a peak position at 0.05 V is shifted by around 100 mV to the lower potential difference values as compared with a positive peak from Fig. 2A attributed to the Ag^+ transfer from the aqueous to the organic phase. This further confirms that the origin of the signals found within the range from -0.2V to 0.2V origin from a mixture of electron and

ion transfer processes. Fig. 2F shows the positive and negative peak currents plotted in function of the added $AgNO_3$ for the signals located at 0 V and -0.1 V, respectively. For fixed Fc concentration in the organic phase, and increasing $AgNO_3$ concentration added to the aqueous phase we have observed two linear dynamic ranges, first up to 500 µM and the second up to the last studied concentration point equal to 2 mM. According to our understanding, for the high Fc excess over Ag^+ the interfacial charge transfer reactions happening within the concerned potential range are mainly governed by the electron transfer between Fc and Ag^+, and Fc^+ crossing the interface. The ratio of the positive (0.704 $A{\cdot}M^{-1}$) and negative (1.331 $A{\cdot}M^{-1}$) slope for the first linear range is equal to 0.5 indicating that more charge is carried on the reverse voltammetry scanning. From [$AgNO_3$] = 500 µM we started observing second linear dynamic range that was attributed to the increasing fraction of current carried by the Ag^+ transfer either from the aqueous to the organic phase or from the organic to the aqueous phase. Also, we cannot exclude the possibility to reduce Ag^+ within the interfacial region on the organic phase side of the liquid-liquid interface by Fc species, as above $\Delta_{org}^{aq}\phi_{Ag^+}$ it will start partitioning to the organic phase (eq. 6). Fig. S2 (see electronic supporting information) shows a photo of the macroscopic cell taken after voltammetric cycling displaying a LLI with a clearly visible thick film presumably being made of Ag NPs. We have also set a control experiments (see photos from Fig. S2), where the flask was filled with the 5 mM $AgNO_3$ and 10 mM Na_2SO_4 (pH = 7) as the aqueous phase and the 10 mM Fc and 5 mM BTPPATPBCl as the organic phase. Already after 5 minutes we started noticing the formation of the precipitate within the interfacial region indicating that the Galvani potential difference of the formed LLI (open circuit potential) is sufficient to drive Ag^+ reduction by Fc from the organic phase.

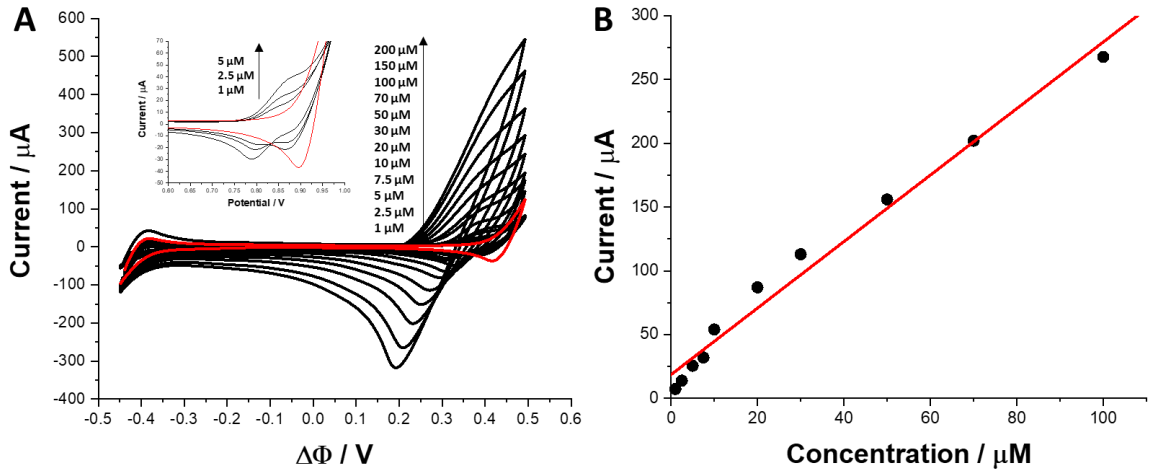

Figure 3. A - Ion transfer voltammograms that were recorded for the increasing concentration of 1,6-DAH (1 – 200 µm) added to the aqueous phase (10 mM Na_2SO_4; pH = 11). The scan rate was 20 $mV{\cdot}s^{-1}$. B – Calibration curve plotted for the positive current signal corresponding to the transfer of 1,6-DAH from the aqueous to the organic phase.

In our previous work, we have shown that interfacial polycondensation of polyamide derived from the reaction between 1,6-DAH and AC can be studied and controlled at the ITIES.[38] Fig. 3A shows the cyclic voltammograms recorded in the presence of 1,6-DAH added to the aqueous phase in the concentration range from 1 to 200 µM. Background subtracted curves are additionally presented as Fig. S3 (see electronic supporting information). At pH = 11, the ratio of monoprotonated (1,6-DAH^{+}) and doubly protonated (1,6-DAH^{2+}) diamines is 1:1 (pK_{a1} = 10.8 and pK_{a2} = 11.9).[38,52] This means that the currents making the signals at $\Delta^{aq}_{org}\phi_{1/2}$ = 0.35V are governed by 1,6-DAH^{+} and 1,6-DAH^{2+} transferring from the aqueous to the organic phase (positive currents) and due to their back transfer (negative currents). Linear increase of the positive peak current plotted in function of the increasing diamine concertation further confirms this behaviour. We have also recorded the cyclic voltammogram in the presence of the background electrolytes and 10 mM AC added to the organic phase (see Fig. S5 from electronic supporting information). No additional signals were recorded within the available potential window. The interfacial reaction between acyl chloride and water molecules leading to the formation of carboxylic groups cannot be excluded. The formation of adipic acid, its partitioning to the aqueous phase where it should exists in the hydrolysed form was not observed during our experiments.

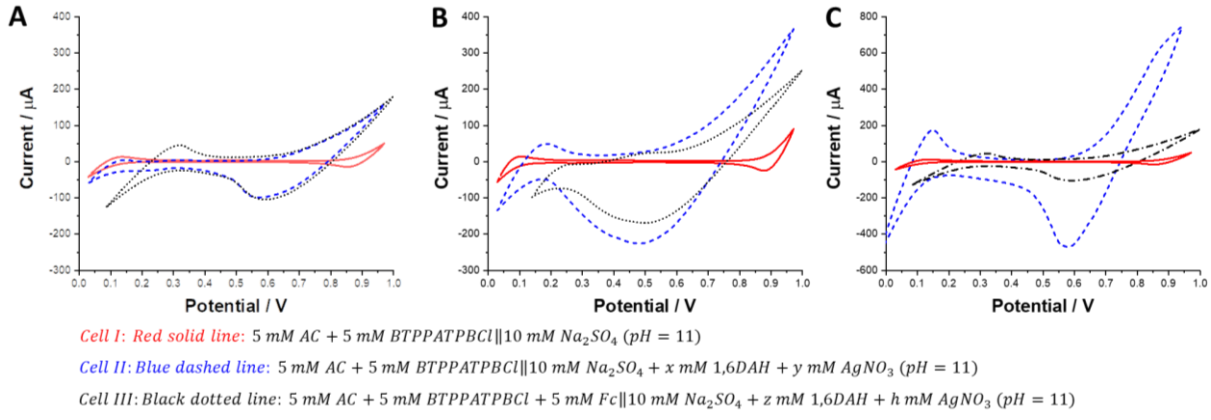

Figure 4. CVs recorded at ITIES under different experimental conditions which are depicted as cell I, II and III. In each section (A, B and C) red solid line corresponds to the cell I. CVs marked as blue dashed line were recorded in cell II with x = 5 mM and y = 0 mM for A; x = 10 mM and y = 0 mM for B; and x = 5 mM and y = 2 mM for C. CVs marked as black dotted line were recorded in cell II for z = 5 mM and h = 2 mM for A; z = 10 mM and h = 2 mM for B; and z = 5 mM and h = 2 mM for C. Scan rate was 20 mV·s^{-1}.

After individual study of all components needed to form polyamide film decorated with Ag-based NPs (at pH higher than 7 we cannot exclude the formation of silver hydroxide and silver oxide) the logical step was to formulate the ITIES composed of all needed reagents. Fig. 4 shows CVs recorded

under different composition of the organic and the aqueous phase. The pH of the later was set to be 11. The major chemical variable of the organic phase was the presence or the absence of 10 mM Fc, whereas for the aqueous phase it was the concentration of 1,6-DAH (either 5 or 10 mM) and the presence of $AgNO_3$. Interestingly, in the presence of 1,6-DAH we did not observe the formation of white or yellow precipitate being AgOH (eq. 7) or Ag_2O (eq. 8), respectively, indicating that silver can be dissolved in the alkaline media at given pH and the aqueous phase composition.

$$Ag^+ + OH^- \rightarrow AgOH \downarrow \quad (7)$$

$$2AgOH \rightarrow Ag_2O \downarrow + H_2O \quad (8)$$

According to the literature survey at relatively high pH and in the presence of compounds holding primary amine groups (in our case 1,6-DAH), AgOH can either dissolve to form silver hydroxy complexes – $Ag(OH)_j^{(j-1)-}$ [53] or can be stabilized in a form of Ag^+ – amine based complex:

$$Ag^+ + H_2N(CH_2)_6NH_2 \rightleftarrows Ag[H_2N(CH_2)_6NH_2]_2^+ \quad (9)$$

The dashed blue curve from Fig. 4A was recorded in the presence of 5 mM 1,6-DAH at pH = 11. The transfer of 1,6-DAH is manifested as a broad signal limiting the potential window on the more positive potential difference side. Further addition of 10 mM Fc to the organic phase and 2 mM $AgNO_3$ to the aqueous phase resulted in the appearance of the additional signal shortening the potential window on the less positive potential side. This is attributed to the interfacial transfer of NO_3^- anions. To our surprise, the intensity of either positive or negative currents for E > 0.65V and E = 0.57V, respectively, in the presence or absence of Ag containing ions (in a form of hydroxy complexes or a complex formed with 1,6-DAH) in the aqueous phase and Fc species in the organic phase remained nearly unaffected. We were expecting to observe additional fraction of current carried by charge transfer reactions discussed above and related to Ag-complex and Fc^+ ion transfer, and Ag-complex reduction. Even more surprising are the data plotted in Fig. 4B with the only difference as comparted with the previously discussed data set (Fig. 4A) being the increased concertation of 1,6-DAH (from 5 mM to 10 mM). First of all, the limiting current on the more positive side of the potential window increased from around 200 µA to 400 µA as the concentration of 1,6-DAH was doubled (see blue, dashed curve in Fig. 4B). Addition of 10 mM Fc to the organic phase and 2 mM $AgNO_3$ to the aqueous phase is marked as the dotted black curve. Again we have noticed NO_3^- transfer on the less positive potential side shortening the available potential window, dropping current on the more positive potential side and a small signal recorded at around E = 0.45 V. The latter can be attributed to either electron transfer reaction related to Ag^+-complex reduction or Fc^+ interfacial transfer formed during the Ag-based NPs formation. Counter intuitive is the drop of the current recorded at E > 0.6 V or the drop of the negative peak with the centre at around 0.45 V. Initially we thought that the polyamide film makes a physical boundary

which inhibits the transfer of small ions across the ITIES and even, function as a spacer between Ag^{+}-complexes and electron donating Fc, which in consequence do not contribute to recorded currents. To further verify this hypothesis, we have added the $AgNO_3$ to the aqueous in the absence of Fc in the organic phase. Obtained results are shown in Fig. 4C as blue dashed curve. Here the concentrations of 1,6-DAH in the aqueous phase and AC in the organic phase were kept constant and were equal to 5 mM. Under such conditions, we are able to form compact polyamide film. Obtained positive signal recorded from 0.5 V to 0.9 V reaches nearly 800 µA and is 4 times higher as compared with the blue dashed curve from Fig. 4A recorded for the same conditions with the only exception being a lack of $AgNO_3$. This clearly means that Ag^{+}-complexes can transfer across the ITIES modified with polyamide film. After Fc addition to the organic phase the currents on the more positive side of the potential window drops (see dotted black line in Fig. 4C) by around 200%. We think that this behaviour is related to the formation of Ag-based NPs within the pinholes of the polyamide film that further inhibit charge transfer reactions across the ITIES. Also, at given pH of the aqueous phase forming polyamide film may be terminated with positively charged primary amine groups which do not react with acyl chloride functionalities of AC. As such, the electrostatic repulsion of positively charged Ag-complex and Fc^{+} is possible.

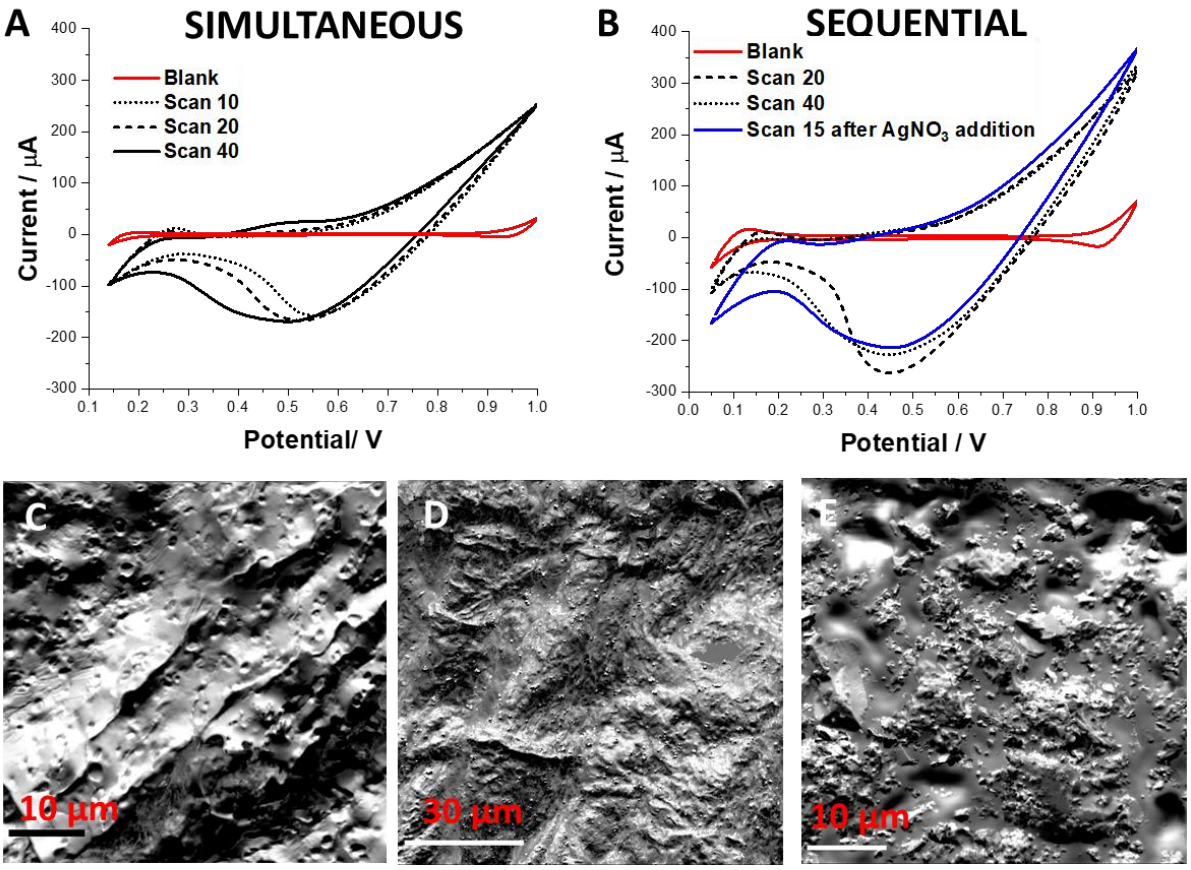

Figure 5. CVs recorded during LLI modification with polyamide and Ag-based NPs through A – simultaneous(Ag-complex reduction during interfacial polycondensation of polyamide film), and B – sequential (interfacial Ag-complex reduction after polymiade film formation) methodology. Red solid line is a blank recorded in cell I (see Fig. 4). Other curves correspond to consecutively recorded CVs (see legend for details). The aqueous phase: 10 mM Na_2SO_4 (pH = 11) with 10 mM 1,6-DAH and 2 mM $AgNO_3$ (added before for A and after for B polyamide film formation). The organic phase: 5 mM BTPPATPBCl with 5 mM AC and 10 mM Fc in 1,2-DCE. Scan rate was 20 $mV \cdot s^{-1}$. SEM micrographs recorded for the polyamide film alone (C), polyamide film decorated with Ag NPs using "simultaneous" methodology (D), and polyamide film decorated with Ag NPs using "sequential" methodology.

We have adopted two methodologies allowing the voltammetric modification of the macroscopic ITIES with polyamide film and Ag-based NPs. In Fig. 5A, the ITIES was modified during 40 consecutively recorded voltammetric scans with all reagents needed to form polyamide film and Ag-based NPs existing in the aqueous (10 mM 1,6-DAH and 2 mM $AgNO_3$) and the organic phase (5 mM AC and 10 mM Fc). In Fig. 5B, during first 40 scans the aqueous phase was deprived from the 2 mM $AgNO_3$. It was added afterwards and 15 more cycles were recorded. We refer to two applied methodologies as simultaneous and sequential, respectively. Obtained voltammetric characteristic are similar to the one already described above (see the discussion pertaining to Fig. 4). Additionally, as shown in Fig. 5A, we have noticed that as we increase the number of voltammetric cycles the width of negative peak increases which may be correlated with the increasing concentration of Fc^+ whose ion transfer currents overlay with all other charge transfer reactions happening in the system. Fig. 5C (see also Fig. S5 from the electronic supporting information) shows the SEM image recorded for the polyamide film collected from the ITIES composed of the 5 mM organic phase electrolyte (BTPPATPBCl) and 5 mM AC used as the organic phase and 10 mM Na_2SO_4 and 10 mM 1,6-DAH used as the aqueous phase. Under such conditions, the film surface appears to be rather homogenous with craters and wrinkles possibly formed during drying process. The appearance of the polyamide film collected directly after recording voltammetric cycle number 40 is shown in Fig. 5A and has changed significantly. Fig 5D and Fig. S6 show that the analysed surface is uniformly decorated with particles assigned as Ag-based objects having a size up to a few tens of nm. We tried to record images with higher magnification but due to polyamide surface charging these attempts were not successful. Fig. 5E and Fig. S7 is the SEM image of a polyamide film prepared via sequential method (Ag NPs formation was done after polyamide film deposition). Here we have found that additional features exiting at the imaged surface were not as homogenous as for the films done according to simultaneous methodology. Fig. S8 represents the IR spectra recorded for polyamide, polyamide synthesized in the presence of ferrocene in the organic phase, and polyamide electrochemically decorated with Ag-based NPs. In all cases, the characteristic

absorption bands (3305, 2934, 2861, 1640, and 1539 cm^{-1}) typical for polyamide were present.[38,54] Eventual presence of ferrocene in the analysed sample can be confirmed based on absorption signals appearing in the region 1100 - 800 cm^{-1} due to out-of-plane vibrations of cyclopentadiene and at around 500 cm^{-1} due to asymmetric tensile vibrations of the metal ring. We have noticed that samples synthesized with ferrocene present in the organic phase and in the absence of $AgNO_3$ in the aqueous phase, provided the highest relative intensity of signals in the region of 1200-1000 cm^{-1}. Also, only for these samples we have observed additional signal at 875 cm^{-1}, which has disappeared in the presence of Ag-based NPs. Since all films formed at the macroscopic ITIES were collected with a rather crude method based on grabbing the deposit with tweezers, we had difficulties in defining the side of the film (either contacting the aqueous or the organic phase), and judging how the process of removing film from the liquid-liquid interface affects its appearance. Proposed workaround is based on using a membrane serving as a support for both, ITIES and formed deposits. In this respect, we have used the fiberglass membrane that was attached to the glass tube with a sealant (see Fig. S9 for details). In this configuration, the organic phase was always in the upper compartment, as such, counteracting possible deposition originating from the sedimentation of the silver oxide particles formed in the volume of the aqueous phase. Again, in the presence of the 1,6-DAH at pH 11 the addition of $AgNO_3$ to the aqueous phase resulted in faint white colour appearance rapidly dissolving after stirring.

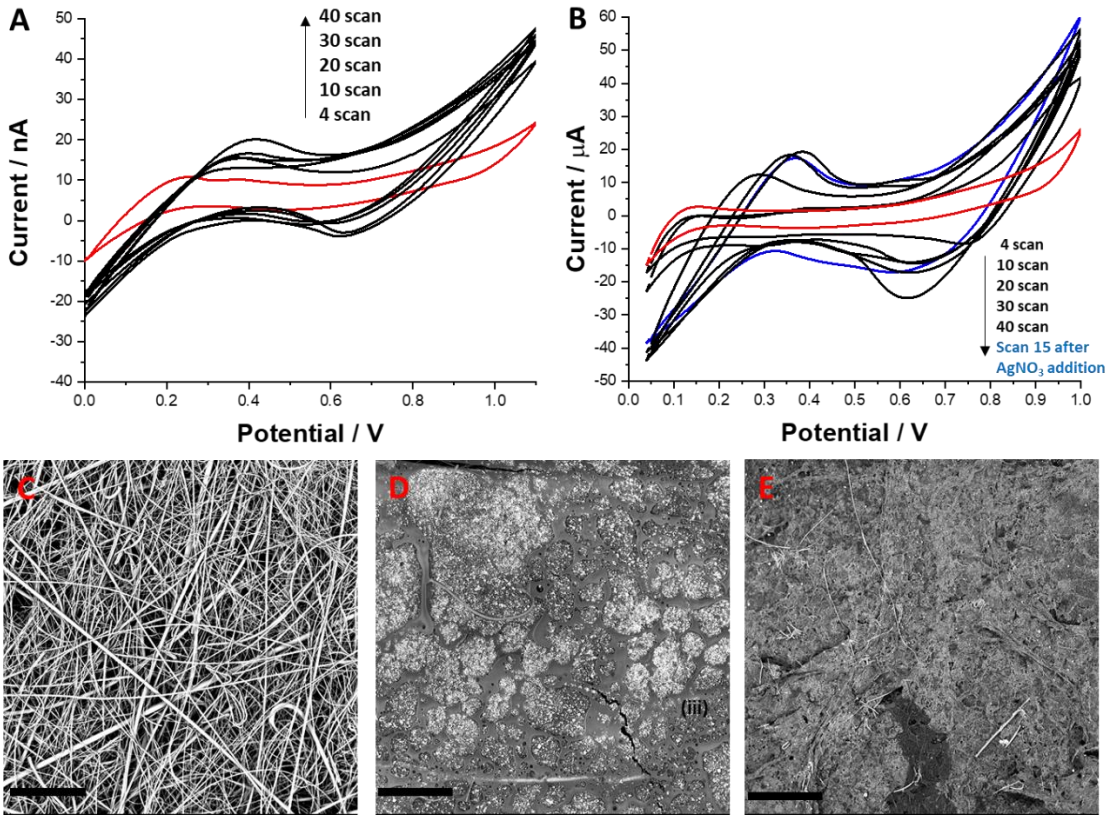

Figure 6. CVs recorded at the ITIES supported with a fiberglass membrane. A - simultaneous (Ag^+ reduction during interfacial polycondensation of polyamide film), and B – sequential (interfacial Ag^+ reduction after polyamide film formation) methodology. Red solid lines correspond to a blank recorded in cell I (see Fig. 4). Other curves correspond to consecutively recorded CVs (see legend for details). The aqueous phase: 10 mM Na_2SO_4 (pH = 11) with 10 mM 1,6-DAH and 2 mM $AgNO_3$ (added before for A and after for B polyamide film formation). The organic phase: 5 mM BTPPATPBCl with 5 mM AC and 10 mM Fc in 1,2-DCE. Scan rate was 20 $mV \cdot s^{-1}$. SEM micrographics recorded for the fiberglass membrane before modification (C), fiberglass membrane modified with polyamide film and Ag NPs formed during simultaneous (D), and sequential (E) modification. For the SEM images: the scale bars correspond to 50 μm.

In Fig. 6 we have plotted the CVs recorded during ITIES supported with a fibre glass membrane modification. Once all reagents needed to form a polyamide film and Ag NPs were present in both phases we have recorded shared voltammetric features: (i) increasing capacitive current; (ii) positive; and (iii) negative limiting currents shifting towards lower and higher potential difference values, respectively. After recording appropriate amount of consecutively recoded CVs the fiberglass membrane were collected and analysed with SEM. Fig. 6C is the membrane composed of a pressed glass fibres before modification. Fig. 6D is a membrane decorated with the polyamide film and Ag NPs collected from the ITIES after recording CVs from Fig. 6A. During interfacial modification, the shown side of the membrane was contacting the aqueous phase. The inspection of the membrane surface with a naked eye revealed the presence of grey surface expected for the forming Ag NPs. These can be further visualized as the island-like domain present within the membrane surface decorated with a number of particles (see Fig. S10A). The situation has changed completely as we move to the fiberglass membrane modified sequentially. The initially formed polyamide film most probably form a compact layer in between the glass fibres which inhibits the formation of Ag NPs. The frequency of occurrence of the corresponding white spots has dropped from clearly visible aggregates (Fig. 6D) to a single and rarely noticeable points distributed among the analysed surface. In future we plan to extend our study focused on electrochemical modification of the interracially formed polyamide film with other nanomaterials. We also plan to investigate the applicability of the form material in textile industry after scaling up the entire platform.

Conclusions

In this work, we have studied the possibility to form polyamide film further decorated with Ag NPs at the electrified liquid-liquid interface. Interfacial polycondensation was controlled via partially protonated 1,6-diaminohexane transfer from the aqueous phase to the LLI where it reacts with adipoyl

chloride. Ag nanoparticleswere form either during interfacial polycondensation of polyamide or after initial polymerization using cyclic voltammetry. As such, the Ag^+ cations initially dissolved in the aqueous phase were reduced to Ag(0) by the electron donating Fc dissolved in the organic phase. All possible charge transfer reactions happening across the electrified liquid-liquid interface were studied individually and later in a complex system (all reagents were placed in the electrochemical cell). Formation of Ag nanoparticles was confirmed with SEM. Polyamide decorated with Ag nanoparticles was formed as a freestanding film at the electrified liquid-liquid interface and within the fiberglass membrane used as a support of both, the liquid-liquid interface and forming deposit.

Conflicts of interest

Authors declare no conflict of interests.

Acknowledgments

The presented research was financed by the National Science Centre Poland as part of the PRELUDIUM 19 project (UMO-2020/37/N/ST4/00270). Magdalena Karpińska is acknowledge for performing initial experiments.

References

[1] J. Koryta, *Electrochim. Acta* **1979**, *24*, 293–300.

[2] F. Reymond, D. Fermin, H. J. Lee, H. H. Girault, *Electochim. Acta* **2000**, *45*, 2647–2662.

[3] K. Rudnicki, L. Poltorak, S. Skrzypek, E. J. R. Sudhölter, *Anal. Chem.* **2018**, *90*, 7112–7116.

[4] Petr Vanysek and Luis Basaez Ramirez, *J. Chil. Chem. Soc.* **2008**, *2*, 1455–1464.

[5] Z. Samec, *Pure Appl. Chem.* **2004**, *76*, 2147–2180.

[6] S. Liu, Q. Li, Y. Shao, *Chem. Soc. Rev.* **2011**, *40*, 2236–53.

[7] G. C. Lillie, R. A. W. Dryfe, S. M. Holmes, *Analyst* **2001**, *126*, 1857–1860.

[8] B. Liu, M. V. Mirkin, *Electroanalysis* **2000**, *12*, 1433–1446.

[9] H. Hu, S. Xie, X. Meng, P. Jing, M. Zhang, L. Shen, Z. Zhu, M. Li, Q. Zhuang, Y. Shao, *Anal. Chem.* **2006**, *78*, 7034–7039.

[10] N. Younan, M. Hojeij, L. Ribeaucourt, H. H. Girault, *Electrochem. Commun.* **2010**, *12*, 912–915.

[11] P. S. Toth, A. K. Rabiu, R. A. W. W. Dryfe, *Electrochem. commun.* **2015**, *60*, 153–157.

[12] M. C. Collins, M. Hébrant, G. Herzog, *Electrochim. Acta* **2018**, *282*, 155–162.

[13] L. Poltorak, A. Gamero-Quijano, G. Herzog, A. Walcarius, *Appl. Mater. Today* **2017**, *9*, 533–550.

[14] P. S. Toth, Q. M. Ramasse, M. Velický, R. A. W. W. Dryfe, *Chem. Sci.* **2015**, *6*, 1316–1323.

[15] B. Sefer, R. Gulaboski, V. Mirčeski, *J. Solid State Electrochem.* **2011**, *16*, 2373–2381.

[16] K. Lepková, J. Clohessy, V. J. Cunnane, *Electochim. Acta* **2008**, *53*, 6273–6277.

[17] A. Trojánek, J. Langmaier, Z. Samec, *J. Electroanal. Chem.* **2007**, *599*, 160–166.

[18] U. Evans-Kennedy, J. Clohessy, V. J. Cunnane, *Macromolecules* **2004**, *37*, 3630–3634.

[19] R. Knake, A. W. Fahmi, S. A. M. Tofail, J. Clohessy, M. Mihov, V. J. Cunnane, *Langmuir* **2005**, *21*, 1001–1008.

[20] M. Vignali, R. Edwards, V. J. Cunnane, *J. Electroanal. Chem.* **2006**, *592*, 37–45.

[21] A. W. Fahmi, S. A. M. Tofail, J. Clohessy, M. Mihov, V. J. Cunnane, N. Ng, **2005**, 1001–1008.

[22] K. Sipa, K. Kowalewska, A. Leniart, S. Skrzypek, L. Poltorak, *Electrochem. Commun.* **2021**, *123*, 106910.

[23] K. Kowalewska, K. Sipa, B. Burnat, S. Skrzypek, L. Poltorak, *Materials (Basel).* **2022**, *15*, 2196.

[24] A. Gamero-Quijano, M. Dossot, A. Walcarius, M. D. Scanlon, G. Herzog, *Langmuir* **2021**, *37*, 4033–4041.

[25] L. Poltorak, M. Hébrant, M. Afsharian, M. Etienne, G. Herzog, A. Walcarius, *Electrochim. Acta* **2016**, *188*, 71–77.

[26] L. Poltorak, G. Herzog, A. Walcarius, *Electrochem. commun.* **2013**, *37*, 76–79.

[27] S. Tan, M. Hojeij, B. Su, G. Meriguet, N. Eugster, H. H. Girault, *J. Electroanal. Chem.* **2007**, *604*, 65–71.

[28] M. D. Scanlon, E. Smirnov, T. J. Stockmann, P. Peljo, *Chem. Rev.* **2018**, *118*, 3722–3751.

[29] A. N. J. Rodgers, R. A. W. Dryfe, **2016**, 472–479.

[30] T. J. Stockmann, J. Zhang, J. C. Wren, Z. Ding, *Electochim. Acta* **2012**, *62*, 8–18.

[31] D. W. M. Arrigan, *Annu. Reports Sect. "C" Physical Chem.* **2013**, *109*, 167.

[32] A. N. J. Rodgers, S. G. Booth, R. A. W. Dryfe, *Electrochem. commun.* **2014**, *47*, 17–20.

[33] M. Arooj, D. W. M. Arrigan, R. L. Mancera, *J. Phys. Chem. B* **2019**, *123*, 7436–7444.

[34] R. Matsui, T. Sakaki, T. Osakai, *Electroanalysis* **2012**, *24*, 1164–1169.

[35] C. J. Collins, C. Lyons, J. Strutwolf, D. W. M. Arrigan, *Talanta* **2010**, *80*, 1993–1998.

[36] D. W. M. Arrigan, M. J. Hackett, R. L. Mancera, *Curr. Opin. Electrochem.* **2018**, *12*, 27–32.

[37] A. Sherburn, M. Platt, D. W. M. Arrigan, N. M. Boag, R. A. W. Dryfe, *Analyst* **2003**, *128*, 1187–1192.

[38] K. Kowalewska, K. Sipa, A. Leniart, S. Skrzypek, L. Poltorak, *Electrochem. commun.* **2020**, *115*, 106732.

[39] J. Guo, T. Takahira, R. Othman, P. R. Unwin, *Electrochem. commun.* **2003**, *5*, 1005–1010.

[40] C. Johans, J. Clohessy, S. Fantini, Kyosti Kontturi, V. J. Cunnane, *Electrochem. Commun.* **2002**, *4*, 227–230.

[41] V. J. Cunnane, G. Geblewicz, D. J. Schiffrin, *Electrochim. Acta* **1995**, *40*, 3005–3014.

[42] N. E. A. Cousens, A. R. Kucernak, *Electrochem. commun.* **2011**, *13*, 1539–1541.

[43] M. Velický, K. Y. Tam, R. A. W. Dryfe, *Anal. Methods* **2012**, *4*, 1207–1211.

[44] T. Kakiuchi, *J. Electroanal. Chem.* **2004**, *569*, 287–291.

[45] Y. Kitazumi, T. Kakiuchi, *J. Electroanal. Chem.* **2010**, *648*, 8–14.

[46] E. Laborda, A. Molina, V. F. Espin, F. Martinez-Ortiz, Jose Gracia de la Torre, R. G. Compton, *Angew. Chemie Int. Ed.* **2017**, *56*, 782–785.

[47] F. Scholz, U. Hasse, *Electrochem. commun.* **2005**, *7*, 541–546.

[48] T. Jane Stockmann, H. Deng, P. Peljo, K. Kontturi, M. Opallo, H. H. Girault, *J. Electroanal. Chem.* **2014**, *729*, 43–52.

[49] B. Su, I. Hatay, A. Trojánek, Z. Samec, T. Khoury, C. P. Gros, J. M. Barbe, A. Daina, P. A. Carrupt, H. H. Girault, *J. Am. Chem. Soc.* **2010**, *132*, 2655–2662.

[50] R. Partovi-Nia, B. Su, F. Li, C. P. Gros, J. M. Barbe, Z. Samec, H. H. Girault, *Chem. - A Eur. J.* **2009**, *15*, 2335–2340.

[51] I. Hatay, B. Su, F. Li, M. A. Méndez, T. Khoury, C. P. Gros, J. M. Barbe, M. Ersoz, Z. Samec, H. H. Girault, *J. Am. Chem. Soc.* **2009**, *131*, 13453–13459.

[52] D. R. Lide, *Handb. Chem. Phys.* **2003**, *53*, 2616.

[53] H. B. Jonassen, T. F. Fagley, C. C. Rolland, P. C. Yates, **1985**, 864–868.

[54] K. Sipa, K. Kowalewska, A. Leniart, A. Walcarius, G. Herzog, S. Skrzypek, L. Poltorak, *Electrochem. commun.* **2021**, *123*, DOI 10.1016/j.elecom.2020.106910.

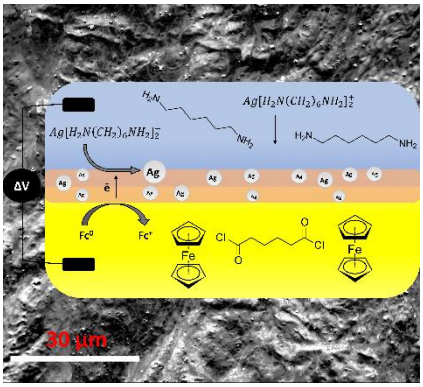

TOC: The electrified liquid-liquid interface is simultaneously modified with polyamide (Nylon-6,6) and silver based particles under electrochemical control. Silver is dissolved in the aqueous phase together with 1,6-diaminohexane (soluble complex is formed), whereas the organic phase is the solution of adipoyl chloride and ferrocene.